



# Cyclic stress responses of a newly developed nickel-base superalloy at elevated temperatures

Luqing Cui <sup>a, b</sup>, Jinjiang Yu <sup>a, \*</sup>, Jinlai Liu <sup>a</sup>, Xiaofeng Sun <sup>a</sup>

<sup>a</sup> Institute of Metal Research, Chinese Academy of Sciences, Shenyang 110016, China

<sup>b</sup> School of Materials Science and Engineering, University of Science and Technology of China, Hefei 230026, China



## ARTICLE INFO

### Article history:

Received 26 March 2018

Received in revised form

13 September 2018

Accepted 21 September 2018

Available online 22 September 2018

### Keywords:

M951G alloy

Low cycle fatigue

Cyclic stress response

Deformation mechanisms

Microstructural degradations

## ABSTRACT

Total strain-controlled low cycle fatigue tests were conducted on the newly designed nickel-base superalloy M951G under different testing conditions; the relationship among cyclic stress responses, microstructural degradations, deformation mechanisms and testing conditions has been established. Results show that both the cyclic hardening and softening behaviors are dependent on the testing temperature and strain amplitude. As the strain amplitude increases both at 900 and 1000 °C, M951G alloy exhibits cyclic hardening under low strain amplitudes and cyclic softening under higher strain amplitudes. At 900 °C, the initial cyclic hardening is related to the coherent  $\gamma/\gamma'$  interface, parallel dislocation arrays and dislocation bypassing the tiny  $\gamma'$  particles. At higher strain amplitudes, the initial cyclic softening is due to the higher density of shearing dislocations in  $\gamma'$  precipitates. At 1000 °C, plenty of parallel dislocation arrays present in  $\gamma$  channels, which reduces the possibility of dislocation interactions from different slip systems and results in initial cyclic hardening. Under higher strain amplitudes, apart from microstructural degradations, dislocations shearing into  $\gamma'$  precipitates and formation of dislocation networks, the dislocation annihilation and partial loss of coherency of  $\gamma'$  precipitates are also responsible for the initial cyclic softening at 1000 °C.

© 2018 Published by Elsevier B.V.

## 1. Introduction

Nickel-base superalloys are widely used as the turbine blades and vanes in the aircraft engines and advanced gas engines, since they have excellent mechanical properties and good corrosion resistance at elevated temperatures [1–9]. The microstructures of superalloys consist of a considerable number of ordered  $\gamma'$  precipitates with  $L1_2$  structure coherently embedded in a disordered solid solution  $\gamma$  matrix with fcc (face centered cubic) structure, which are responsible for the outstanding performances of superalloys [10–12].

In previous studies, the influences of temperature and applied stress on the properties of superalloys have been widely reported, such as tensile [13–15] and creep properties [3,8,16,17]. However, in practical application, the hot section components of engines are subjected to cyclic thermal stresses resulting from startup and shutdown. Especially in the transient temperature gradients, thermal strains and stresses are applied on the blades. Therefore,

compared with tensile and creep deformations, low cyclic fatigue (LCF) can approach the real conditions of these superalloys during service, and the damage of superalloys can be evaluated accurately. Thus, isothermal LCF is often used to predict damage behavior and fatigue life.

In the past several decades, much work has been done on the cyclic stress responses and deformation mechanisms of superalloys, including the effects of strain rate [18–21], strain amplitude [22–24], testing temperature [25–27], frequency [28,29], loading waveform [30] and thermal gradient [31–34] on fatigue performances, among which testing temperature and strain amplitude are of special interest [23,35–41]. Chu studied the LCF behavior of DZ951 alloy under different testing conditions [42], results showed that cyclic hardening was observed at 700 °C as the consequence of high-density of slip bands and tangled dislocations in microstructures. However, at 900 °C, the alloy exhibited cyclic softening under higher strain amplitudes caused by the loss of coherency of  $\gamma'$  precipitates [43] and cyclic stability under low strain amplitudes due to the precipitation of fine second carbides. Research from Liu demonstrated that for [011] oriented nickel-base single crystal superalloy at 980 °C, with the increase of strain amplitude the alloy

\* Corresponding author.

E-mail address: [jjyu@imr.ac.cn](mailto:jjyu@imr.ac.cn) (J. Yu).

displays a transition from initial cyclic hardening at the total strain amplitude of 0.5% to cyclic softening at the total strain amplitude of 2.0% [44]. In addition, the effects of temperature on the dislocation and slip band motion were also discussed [37,45,46]. At low temperature, slip bands consisting of shearing dislocations in  $\gamma'$  precipitates on the {111} slip planes were the primary slip features [45,46] during fatigue deformation. Nevertheless, as the temperature increases the deformation became much homogeneous and the density of dislocations was much lower [37]. Similar dislocation configurations also reported in Ref. [46] that slip bands were the main slip characteristics at 500 and 750 °C, but when the temperature increases, the extend of invasion and extrusion became weak. Apart from that, during cyclic loading the microstructural evolutions such as the average size and morphology of  $\gamma'$  precipitates, the coherent relationship between  $\gamma$  and  $\gamma'$  phases as well as the density and configuration of dislocations also change with the number of cycles increasing. Correspondingly, these changes will also have a significant effect on the fatigue properties of superalloys [47,48].

As mentioned above, although a great deal of investigations on LCF behaviors of superalloys have been performed, the relationship among cyclic stress responses, microstructural degradations, deformation mechanisms and testing conditions is still unclear. Especially, the fatigue deformations of polycrystalline superalloys at high temperatures need to be further studied. It will certainly be helpful for better understanding of cyclic stress response of superalloys. In present study, the newly designed nickel-base

superalloy M951G is chosen to investigate the effects of testing conditions on the cyclic stress response behavior of superalloy at 900 and 1000 °C. Furthermore, attentions are paid to the corresponding microstructural degradations and deformation mechanisms to establish a clear microstructure-fatigue property relationship.

## 2. Materials and experimental procedures

The nominal chemical composition of M951G alloy used in this study is listed in the Table 1. The master alloy was remelted in a vacuum induction furnace and the mold preheating and pouring temperatures were 900 and 1450 °C, respectively. For all LCF samples, the procedure of heat treatment was the following: 1210 °C × 4 h, AC → 1100 °C × 4 h, AC → 870 °C × 24 h, AC (AC: air cooling).

After heat treatment, the precipitated phases of M951G alloy are observed by an INSPECT F50 scanning electron microscope (SEM) and a JEM 2100 transmission electron microscope (TEM). The INSPECT F50 SEM was equipped with an Oxford energy dispersive spectrometer (EDS), which was used to qualitatively identify the chemical compositions of precipitated phases in M951G alloy. Fig. 1a and b show the typical  $\gamma/\gamma'$  morphologies of M951G alloy after heat treatment, which consist of coarse cuboidal  $\gamma'$  precipitates with an average size of 420 nm, separated by narrow  $\gamma$  matrix channels of about 80 nm mean width. In addition, a considerable number of tiny spherical  $\gamma'$  precipitates with a mean diameter of about 70 nm also have been observed in  $\gamma$  matrix channels, as shown in Fig. 1a and b. On the other hand, both the large block-like carbides in interdendritic regions (Fig. 1c) and fine chain-like carbides along the grain boundaries (Fig. 1d) were identified to be rich in Hf and Nb by EDS, as presented in Fig. 1e. Furthermore, X-ray diffraction (XRD) patterns of M951G alloy after heat treatment are displayed in Fig. 1f, which provides three groups

**Table 1**  
Nominal composition of M951G alloy (wt%).

W	Mo	Nb	Co	Cr	Al	Hf	others	Ni
6.5	3	2.2	5	9	6	1.5	0.091	Bal

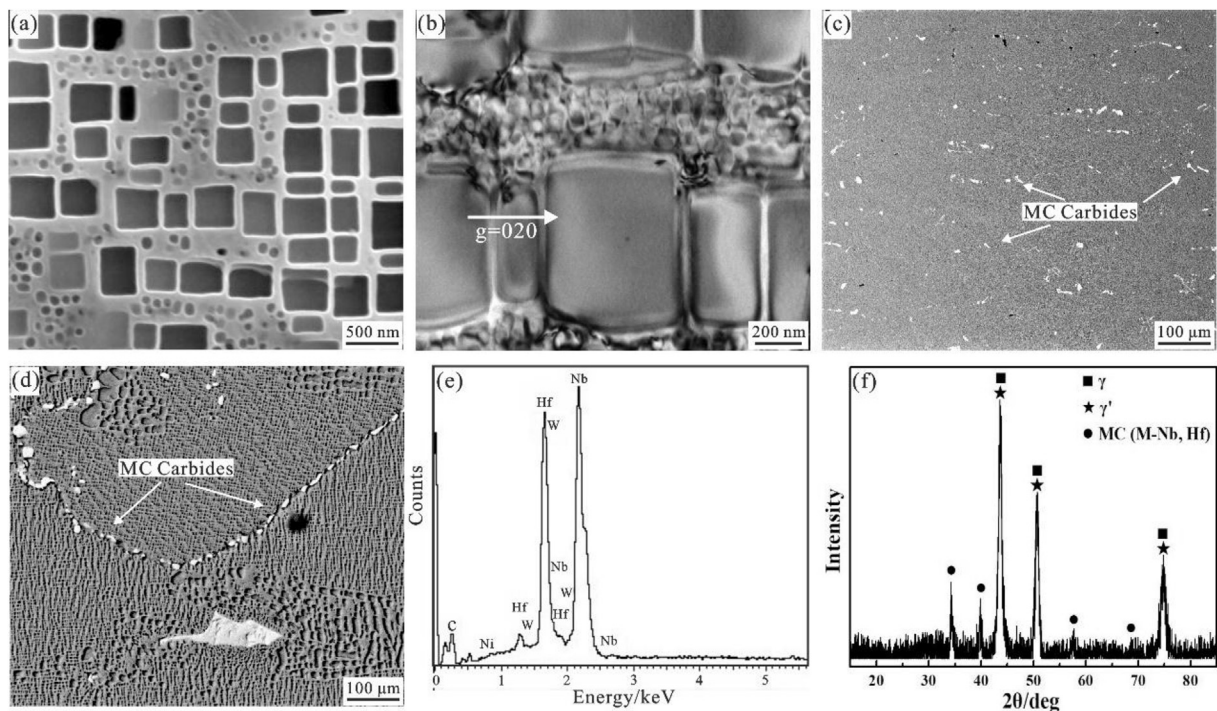


**Fig. 1.** Precipitated phases of M951G alloy after heat treatment. (a)–(b) Typical morphologies of coarse cuboidal and fine spherical  $\gamma'$  precipitates observed by SEM and TEM, respectively. TEM image was taken close to the [001] zone axis. (c) Large and block-like carbides precipitated in the interdendritic region. (d) Fine and chain-like carbides precipitated along the grain boundaries. (e) EDS spectrum of carbides. (f) XRD patterns of M951G alloy after heat treatment.

Download English Version:

<https://daneshyari.com/en/article/11019960>

Download Persian Version:

<https://daneshyari.com/article/11019960>

[Daneshyari.com](https://daneshyari.com)